Preparation of hydroxyapatite ceramics by hydrothermal hot-pressing method at 300 °C

Junguo Li · Toshiyuki Hashida

Abstract Hydroxyapatite (HA) ceramics were prepared by a hydrothermal hot-pressing (HHP) method at a low temperature (300 °C). DCPD ($CaHPO_4 \cdot 2H_2O$) + $Ca(OH)_2$, OCP ($Ca_8H_2(PO_4)_6 \cdot 5H_2O$) + Ca$(OH)_2$, DCPD + $NH_3 \cdot H_2O$, OCP + $NH_3 \cdot H_2O$ or α-TCP ($Ca_3(PO_4)_2$) + $NH_3 \cdot H_2O$ were used as the precursors. The mixture was treated by HHP under a condition of 300 °C/40 MPa. In sample DCPD + Ca$(OH)_2$ and OCP + $Ca(OH)_2$, the HA ceramics obtained showed a porous and homogenous microstructure, and the bending strength were 9.9 MPa and 10.9 MPa, respectively. In sample α-TCP+$NH_3 \cdot H_2O$, rod-like HA crystals produced. When the starting materials were DCPD + $NH_3 \cdot H_2O$, OCP + $NH_3 \cdot H_2O$, the HA particles produced exhibited plate-like features. It appeared that the plate-like HA particles stacked into a lamellar structure. The formation of the lamellar structure leads to a noticeable improvement in fracture property of the HA ceramic. The bending strength and the fracture toughness of the sample prepared from OCP and ammonia water reach 90 MPa and 2.3 MPam$^{1/2}$, respectively.

J. Li · T. Hashida
Fracture and Reliability Research Institute, Graduate School of Engineering, Tohoku University, Sendai 980-8579, Japan

J. Li (✉)
State Key Laboratory of Advanced Technology for Materials Synthesis and Processing, Department of Materials Science, Wuhan University of Technology, 122 Luoshi Road, Hongshan, Wuhan, Hubei Province 430070, China
e-mail: lijg000@126.com

Introduction

Hydroxyapatite (HA, $Ca_{10}(PO_4)_6(OH)_2$) is a particularly attractive material for human hard tissue implantation due to its excellent biocompatibility [1]. Dense HA ceramics is conventionally prepared by sintering HA powder at high temperatures (>1,000 °C) [2–8]. To improve the poor mechanical properties of dense pure HA ceramics, which possess a bending strength between 90 and 106 MPa and a fracture toughness within 1.0 MPam$^{1/2}$ [9, 10], various substances have been added, including HA, SiC or Si_3N_4 whiskers [1, 11], Al_2O_3, Ni_3Al, PSZ, TZP or Ti_3SiC_2 particles [12–17], and Al_2O_3 platelets [18, 19]. In this way, the strength and toughness are improved to 80–300 MPa and 1.0–3.2 MPam$^{1/2}$, respectively. But the addition of the bioinert materials causes another problem: the biocompatibility of the HA composites will greatly decrease. At the same time, the high sintering temperatures (>1,000 °C) may lead to decomposition of HA and exaggerated grain growth, which will also degrade the biocompatibility and mechanical properties of HA ceramics [20]. The decomposition of HA, and its consequent decrease in biocompatibility as well, is avoided when low temperature preparation techniques are used, such as hydrothermal hot-pressing (HHP) method, calcium phosphate cement, dual-phase mixing. However, the HA ceramics prepared at low temperatures is porous, with a strength of 10–18 MPa [21–25].

Another way to improve the mechanical property of HA bioceramics is to fabricate HA/polymer composites [26–30]. The HA/polymer composites exhibit good mechanical property, with a bending strength of 44–280 MPa and a fracture toughness parallel to cortical

bone. Unfortunately, there are several reports of the toxicity of their biodegradation products [31, 32].

The formation of a lamellar structure will effectively improve the fracture property of materials, and this is well illustrated by the structure of shells. With a lamellar structure composed of calcium carbonate and a small amount of organic substance, shells show the strength and fracture energy about 10 times and 2,000 times greater than those of calcium carbonate (argonite), respectively [33, 34]. It is expected that the formation of lamellar structure in HA ceramics will improve the fracture property. Lamella is commonly stacked by plate-like crystals. Thus, in this work, DCPD ($CaHPO_4 \cdot 2H_2O$) and OCP ($Ca_8H_2(PO_4)_6 \cdot 5H_2O$), whose crystals are plate-like particles, are selected as the precursors, together with $Ca(OH)_2$ or ammonia water, to form HA. In the previous work [35], α-TCP was reported to prepare plate-like OCP in ammonia. In this work, it is investigated whether α-TCP may react with ammonia to produce plate-like, and consequently lamellar HA ceramics.

Experimental procedure

Synthesis of DCPD and OCP

To synthesize DCPD powder, Calcium Nitride ($Ca(NO_3)_2$) solution (1 mol/L, 349 mL) was gradually added to ammonium hydrogen phosphate (($NH_4)_2$ HPO_4, 1 mol/L, 500 mL). The whole process went on with continuous stirring and dripping of ammonia water (~16.5 mol/L) to keep the pH value above 8.0. When the addition of $Ca(NO_3)_2$ ended, absolute acetic acid was dripped in to decrease the pH value to 6.0. The suspension was stirred continuously for 12 h, then the precipitation was washed by de-ionized water and acetone, and dried at 50 °C.

OCP powders were synthesized by hydrolysis of α-TCP (Taihei Chemical Co., Japan) by means of a wet-chemical processing [35]. The buffer solution used in this processing was prepared by mixing 6 mL of 1 N CH_3COONa with 114 mL of 1 N CH_3COOH, followed by diluting the mixture to 600 mL. The buffer solution was put into a 1,000 mL beaker. Then 20.67 g of α-TCP powder was suspended in the previous buffer solution. The vessel was quickly moved into a 70 °C water bath and mechanically stirred. At the same time a plastic wrap was employed to cover the beaker. After 6 h, the solid products were separated with a filter and washed for three times with de-ionized water. Afterwards, the products were dried at 50 °C for 24 h.
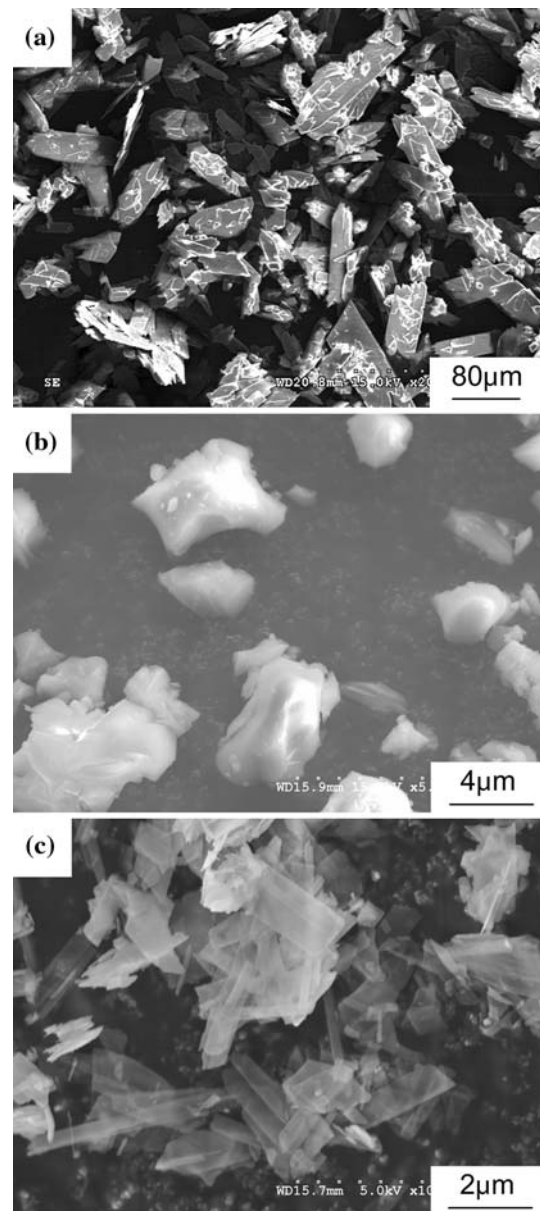

Fig. 1 SEM photographs of (**a**) DCPD, (**b**) α-TCP and (**c**) OCP

The morphologies of the DCPD, OCP and α-TCP were observed with a scanning electron microscope (SEM). As shown in Fig. 1, the shape of the DCPD and OCP crystals is plate-like, while the α-TCP exhibits irregular shapes.

Preparation of HA ceramics and properties evaluation

Figure 2 shows the autoclave used for hydrothermal hot-pressing. The main body of the autoclave has a piston–cylinder structure with an inside diameter of 20 mm. The starting powders are placed in the middle
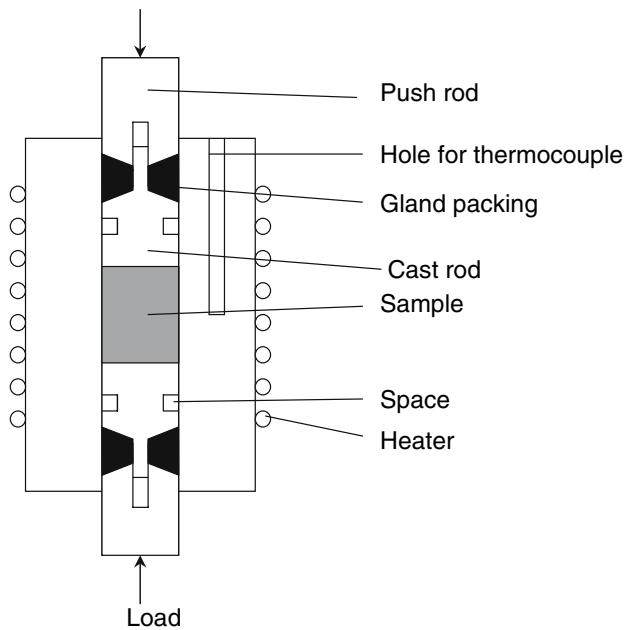
Fig. 2 Schematic illustration of the autoclave for hydrothermal hot-pressing

of the chamber and compressed through push rods and cast rods from top and bottom by applying mechanical pressure. The gland packing between the cast rod and the push rod can deform under pressure to prevent leakage of water. Each cast rod has a space for water retreat, which is set to maintain the appropriate hydrothermal condition. For heating, the autoclave is surrounded by a heater.

DCPD or OCP powder was mixed with $Ca(OH)_2$ in the Ca/P ratio of chemical stoichiometric HA. The mixture (5 g) was placed in the autoclave, and then distilled water (0.5 g) was dripped in, followed by the application of a pressure of 40 MPa. After 3 min, the sample was heated to 300 °C at a heat rate of 10 °C/min and then kept at 300 °C, 40 MPa for 2 h. When the temperature naturally went down to the room temperature, the sample was taken out from the autoclave and dried at 50 °C for 24 h.

With the starting materials containing ammonia water, the DCPD, OCP or α-TCP powder (5 g) was firstly placed in the autoclave, and then ammonia water 0.5 g (28–30 mass% NH_3) was dripped in, followed immediately by HHP treatment to prevent the leakage of NH_3. The HHP conditions were the same as that described previously. The density of the sample was determined by Archimedes method. Sixteen specimens were used to evaluate the bending strength and the fracture toughness by conducting 3-point-bending tests on an Instron material-testing system (Model 1185). The dimension of the samples was 3 mm(width) ×

3 mm(height) × 15 mm(length). A notch of 1.5 mm depth was introduced to eight specimens to evaluate toughness. The loading direction for the 3-point-bending tests was the same as the orientation of the axial stress in the HHP process. The crosshead speed was 0.5 mm/min. The bending strength σ_b and the fracture toughness K_{Ic} were calculated by the following equations [36]:

$$\sigma_b = \frac{3PL}{2bh^2} \qquad (1)$$

$$K_{Ic} = 2.66 \frac{PL}{bh^{3/2}} \qquad (2)$$

where, P is the maximum load, L is the span (=12 mm), b the width of the sample (=3 mm), and h the height of the sample (=3 mm).

The phase of the solidified body was determined by X-ray diffraction (XRD), with $CuK\alpha$ at 40 kV, 40 mA. The morphology of the fracture surface after bending test was observed by means of an SEM.

Results and discussion

The XRD patterns and SEM photographs of the solidified bodies fabricated from DCPD + $Ca(OH)_2$ (hereafter, designated as DC) and OCP + $Ca(OH)_2$ (designated as OC) are presented in Figs. 3 and 4. The HA (PDF: 09–0432) is the unique phase of the solidified bodies, suggesting that the pure HA has been fabricated. In sample DC, the original large DCPD grain sheets have disappeared, replaced by fine spherical HA particles instead (Fig. 4a), which
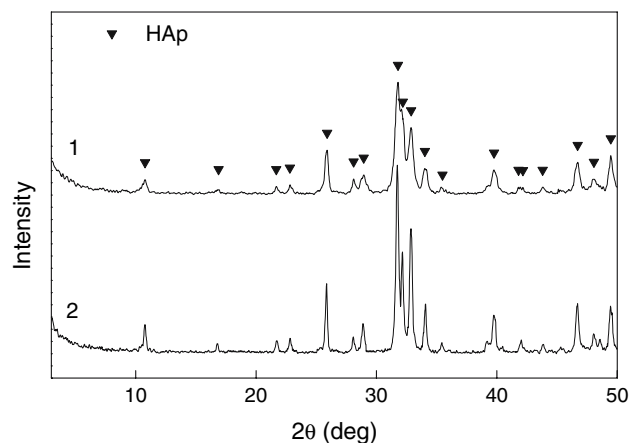
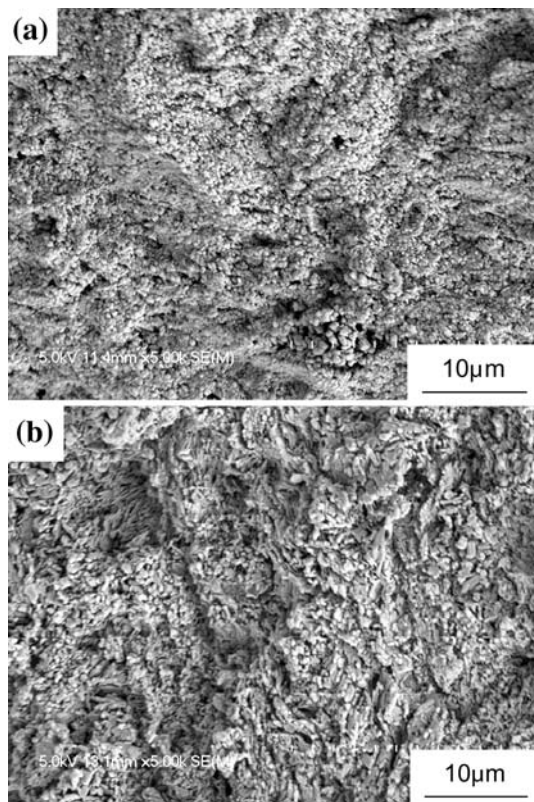**Fig. 3** XRD patterns of samples (**1**) DCPD + $Ca(OH)_2$ (DC) and (**2**) OCP + $Ca(OH)_2$ (OC)
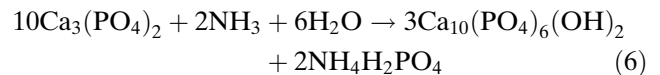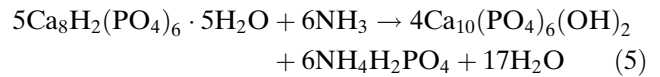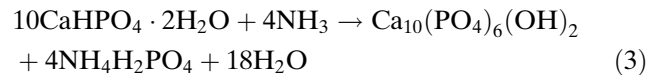
Fig. 4 SEM photographs of the samples (**a**) DCPD+Ca(OH)$_2$ (DC) and (**b**) OCP + Ca(OH)$_2$ (OC)

shows a porous and homogeneous structure. The XRD results also show that the peaks of the HA produced is wide, indicating that the HA grains are fine. In sample OC, most HA crystals are plate-like and distribute randomly. The density of sample DC and OC are 1.74g/cm^3 and 1.81 g/cm^3, respectively. The low relative density (55% and 57%) leads to low bending strengths (9.9 MPa and 10.9 MPa, respectively). The relative density and the bending strength of sample DC are almost the same as that of the HA prepared by HHP at 150 °C [21]. These results indicate that increasing the treatment temperature up to 300 °C causes no further densification and strength development. From the SEM photographs of the fracture surfaces, it can be seen that both sample DC and OC show no lamellar structure, indicating that the addition of Ca(OH)$_2$ is ineffective for the formation of lamellar structure.

Figure 5 shows the XRD patterns of the solidified bodies fabricated from DCPD+NH$_3$ (designated as DN), OCP+NH$_3$ (designated as ON) and α-TCP+NH$_3$ (designated as TN). Except sample DN, whose products contain HA and DCP (PDF: 09-0080), HA is the unique phase of the solidified bodies. For these samples, NH$_4$H$_2$PO$_4$ (PDF: 37-1479) is detected by XRD

on the cast rods (Fig. 6). These results show that the following reactions occur during the HHP process:

$$10CaHPO_4 \cdot 2H_2O + 4NH_3 \rightarrow Ca_{10}(PO_4)_6(OH)_2 \\ + 4NH_4H_2PO_4 + 18H_2O \tag{3}$$

$$CaHPO_4 \cdot 2H_2O \rightarrow CaHPO_4 + 2H_2O \tag{4}$$

$$5Ca_8H_2(PO_4)_6 \cdot 5H_2O + 6NH_3 \rightarrow 4Ca_{10}(PO_4)_6(OH)_2 \\ + 6NH_4H_2PO_4 + 17H_2O \tag{5}$$

$$10Ca_3(PO_4)_2 + 2NH_3 + 6H_2O \rightarrow 3Ca_{10}(PO_4)_6(OH)_2 \\ + 2NH_4H_2PO_4 \tag{6}$$

In sample DN, the amount of the ammonia added is insufficient to react completely with the DCPD, resulting in the remnant of DCP. In sample ON and TN, the amount of the ammonia added exceeds the chemical stoichiometric ratio and can react completely with the calcium phosphates, producing HA and NH$_4$H$_2$PO$_4$. Because the treatment temperature of 300 °C is higher than the melting point of NH$_4$H$_2$PO$_4$, 190 °C [37], NH$_4$H$_2$PO$_4$ will melt and be pushed out under compression during the HHP treatment. Therefore, NH$_4$H$_2$PO$_4$ is not detected by XRD in the solidified bodies and only HA ceramics are obtained.

Figure 7 shows the properties of sample DN, ON and TN. The densities of the three samples are 2.66 g/cm^3, 2.87 g/cm^3 and 2.72 g/cm^3, respectively. The corresponding relative densities are 87%, 91% and 86%, respectively. These values are noticeably higher
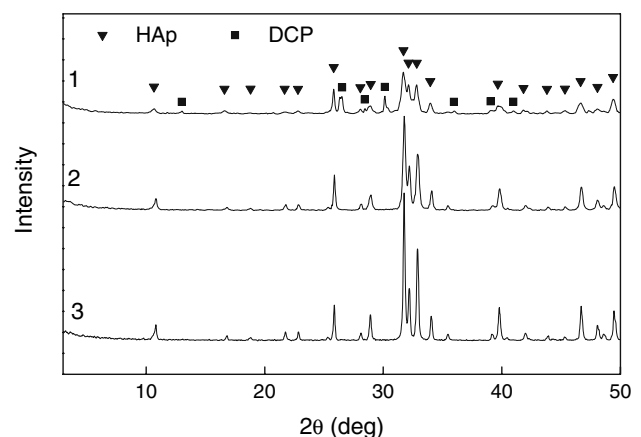

Fig. 5 XRD patterns of samples (**1**) DCPD + NH$_3$ (DN), (**2**) OCP + NH$_3$ (ON), and (**3**) α-TCP+NH$_3$ (TN)
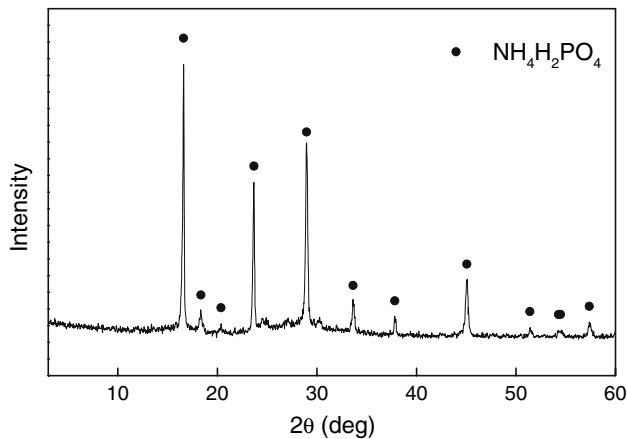
Fig. 6 XRD pattern of the substance crystallized on the cast rods

than those of sample DC and OC. This result indicates that the addition of ammonia water enhances the densification of HA ceramics. It is supposed that $NH_4H_2PO_4$ plays an important role in the densification. As described previously, $NH_4H_2PO_4$ exists as a liquid phase in sample DN, ON and TN during HHP process. The liquid phase has strong influence on grain rearrangement [8] and then enhances the densification of HA. As shown in Fig. 7, the bending strength and the fracture toughness of sample ON exhibit the highest values, suggesting that OCP is the most suitable material to prepare HA ceramics with high mechanical property. No data is available for sample DN, because the prepared samples contained large defects and broke into several pieces in the machining process.

The SEM photographs of sample DN, ON and TN are presented in Fig. 8. The shape of the HA crystals in sample ON is plate-like (Fig. 8b-1), and the plate-like crystals are observed stack into a lamellar structure (Fig. 8b). The microstructure of sample DN is similar to sample ON. Due to the weak interlayer interaction

force, sample DN breaks into several pieces during the machining process. In sample TN, the HA particles produced show a rod-like feature. These results indicate that only plate-like crystals are favorable to form a lamellar structure. The high bending strength and fracture toughness of sample ON may be attributed to the lamellar structure, suggesting that the formation of lamellar structure is effective to improve the fracture properties of HA ceramics.

When the treatment time prolongs to 4 h, the bending strength and the fracture toughness of sample ON reach 90 MPa and 2.3 $MPam^{1/2}$, respectively. The bending strength is comparable to the HA ceramics sintered at high temperatures and the fracture toughness is significantly higher (Table 1). These results suggest that it is a feasible way to improve the mechanical properties of HA bioceramics by preparing HA with a lamellar structure by HHP at low temperatures.

Summary

HA ceramics were prepared from various precursors: $DCPD + Ca(OH)_2$, $OCP + Ca(OH)_2$, $DCPD + NH_3 \cdot H_2O$, $OCP + NH_3 \cdot H_2O$ or $\alpha\text{-TCP} + NH_3 \cdot H_2O$. The mixture was treated by hydrothermal hot-pressing method under a condition of 300 °C/40 MPa. The results can be summarized as follows.

When the starting materials contain $Ca(OH)_2$, the shape of the HA particles produced are mainly spherical. The HA ceramics show a porous and homogenous microstructure. The low relative density leads to low bending strengths (9.9–10.9 MPa).

Ammonia water can react with DCPD, OCP and α-TCP to produce HA and $NH_4H_2PO_4$. The HA crystals produced from $DCPD + NH_3 \cdot H_2O$, $OCP + NH_3 \cdot H_2O$ are plate-like, while rod-like HA crystals for $\alpha\text{-TCP} + NH_3 \cdot H_2O$. $NH_4H_2PO_4$ enhances the densification of HA ceramics and contributes to the lamellar

Fig. 7 Properties of the samples DCPD + NH₃ (DN), OCP + NH₃ (ON), and α-TCP + NH₃ (TN)
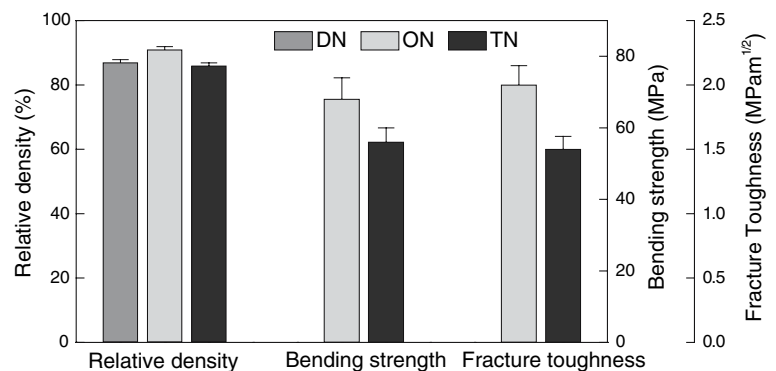
Fig. 8 Fracture surface SEM photographs of samples (**a**) DCPD + NH$_3$ (DN), (**b**) OCP + NH$_3$ (ON), and (**c**) α-TCP+NH$_3$ (TN). (**b-1**, observed on the fracture surface that normal to the loading direction)
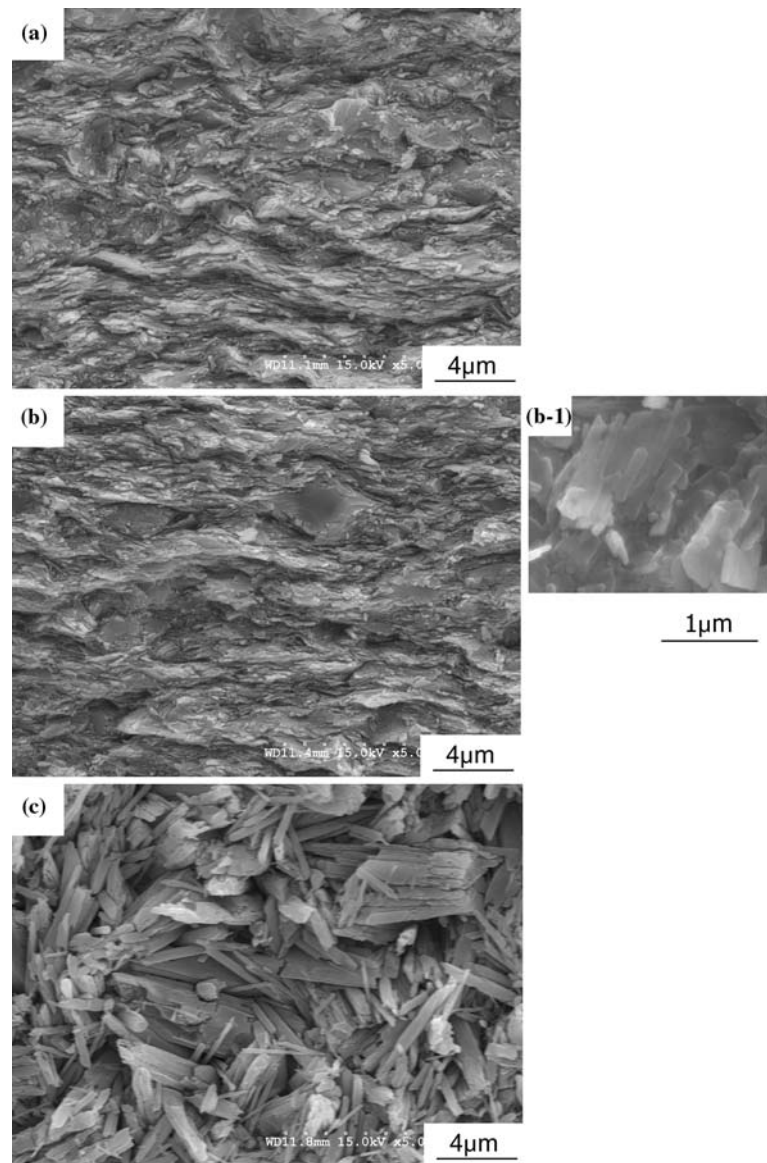

Table 1 Summary of the properties of pure HA ceramics

Reference	Relative density (%)	Strength (MPa)	Fracture toughness (MPam$^{1/2}$)	Synthetic route
Present work	91	68	2.0	HHPed OCP + NH$_3$ at 300 °C for 2 h
	93	90	2.3	HHPed OCP + NH$_3$ at 300 °C for 4 h
Lu [4]	96	90		Sintered HA powder at 1,300 °C for 3 h
Vananduyt [3]	94		0.72	Sintered HA powder at 1,200 °C for 3 h
Akao [2]	94	106		Sintered HA powder at 1,250 °C for 3 h
De with [9]	94	90	1.0	Sintered HA powder at 1,225 °C for 6 h
Choi [10]		100	0.7	Hot pressed HA powder at 1,100°C for 1 h

structure formation from the plate-like HA crystals. The lamellar structure and the rod-like structure improve the fracture property, while the former is more effective.

OCP is the most suitable material to form lamellar structure in HA ceramics by hydrothermal hot-pressing method. The bending strength and fracture toughness of the sample prepared from OCP and ammonia water

under the condition of 300°C/40 MPa/4 h reach 90 MPa and 2.3 MPam$^{1/2}$, respectively.

References

1. Suchanek W, Yoshimura M (1998) J. Mater. Res. 1:94
2. Akao M, Aoki H, Kato K (1981) J Mater Sci 16:809. Doi: 10.1007/BF00552220
3. Vanlanduyt P, Li F, Keustermans JP, Streydio JM, Delannay F, Munting E (1995) J Mater Sci Mater Med 6:8
4. Lu H, Qu Z, Zhou Y (1998) J Mater Sci Mater Med 9:583
5. Murray MGS, Wang J, Ponton CB, Marquis PM (1995) J Mater Sci 30:3061. Doi: 10.1007/BF01209218
6. Goto T, Wakamatsu N, Kamemizu H, Iijima M, Doi Y, Moriwaki Y (1991) J Mater Sci Mater Med 2:149
7. Halouani R, Assolant DB, Champion E, Ababou A (1994) J Mater Sci Mater Med 5:563
8. Suchanek W, Yashima M, Kakihana M, Yoshimura M (1997) Biomaterials 18:923
9. De with G, Vandijk HJA, Hattu N, Prijs K (1981) J Mater Sci 16:1592. Doi: 10.1007/BF00553971
10. Choi JW, Kong YM, Kim HE (1998) J Am Ceram Soc 81[7]:1743
11. Suchanek W, Yashima M, Kakihana M, Yoshimura M (1997) J Am Ceram Soc 80:2805
12. LeGeros RZ (1981) Prog Crystal Growth Charact 4:1
13. Takagi M, Mochida M, Uchida N, Saito K, Uematsu K (1993) J Mater Sci Mater Med 4:50
14. Matsuno T, Watanabe K, Ono K, Koishi M (1996) J Ceram Soc Jap 104:845
15. Ahn ES, Gleason NJ, Ying JY (2005) J Am Ceram Soc 88:3374
16. Kim Hae-Won, Kong Young-Min, Koh Young-Hag, Kim Hyoun-Ee, Kim Hyun-Man, Jea Seung Ko (2003) J Am Ceram Soc 86:2019
17. Sui Lin Shi, Wei Pan, Ming Hao Fang, Zhen Yi Fang (2006) J Am Ceram Soc 89:743
18. Champion E, Gautier S, Bernach-Assollant D (1996) J Mater Sci Mater Med 7:125
19. Gautier S, Champion E, Bernach-Assollant (1999) J Mater Sci Mater Med 19:533
20. Ruys AJ, Wei M, Sorrell CC, Dickson MR, Brandwood A, Milthorpe BK (1995) Biomaterials 16:409
21. Hosoi K, Hashida T, Takahashi H, Yamasaki N, Korenaga T (1996) J Am Ceram Soc 79:2771
22. Onoki T, Hosoi K, Hashida T (2001) In Proceedings of Asia Pacific conference on fracture and strength'01 and International Conference on Advanced Technology in Experimental Mechanics'01, Sendai, October, p 511
23. Martin RI, Brown PW (1995) J Mater Sci Mater Med 6:38
24. Miyamoto Y, Ishikawa K, Fukao H, Sawada M, Nagayama M, Kon M, Asaoka K (1995) Biomaterials 16:855
25. Shi Hong Li, de Wijn JR, Pierre Layrolle, Klaas de Groot (2003) J Am Ceram Soc 86:65
26. Bonfield W (1988) J Biomed Eng 10:522
27. Sinha A, Nayar S, Agrawal A, Bhattacharyya D, Ramachandrarao P (2003) J Am Ceram Soc 86:357
28. Greish YE, Brown PW (2002) J Am Ceram Soc 85:1738
29. Liming Fang, Yang Leng, Ping Gao (2006) Biomaterials 27:3701
30. Greish YE, Bender JD, Lakshmi S, Brown PW, Allcock HR, Laurencin CT (2005) Biomaterials 26:1
31. Athanasiou KA, Niederauer GG, Agrawal CM (1996) Biomaterials, 17:93
32. Ignatius AA, Claes LE (1996) Biomaterials, 17:831
33. Jackson AP, Vincent JFV, Briggs D, Crick RA, Davies SF, Hearn MJ, Turner RM (1986) J Mater Sci Lett 5:975
34. Jackson AP, Vincent JFV, Turner RM (1990) J Mater Sci 25:3173. Doi: 10.1007/BF00587670
35. Nakahira A, Aoki S, Sakamoto K, Yamaguchi S (2001) J Mater Sci Mater Med 12:793
36. Testing Methods for Fracture Toughness of Fine Ceramics, Japanese industrial standard, JIS R 1607–1995
37. Lide D (2000) Handbook of chemistry and physics, 83rd edn. CRC press